

Contents lists available at [ScienceDirect](http://ScienceDirect)

# Materials Science in Semiconductor Processing

journal homepage: [www.elsevier.com/locate/mssp](http://www.elsevier.com/locate/mssp)

## Optical properties of $\text{Si}_x\text{Ge}_{1-x}$ single crystals grown by liquid phase diffusion

Hüseyin Derin <sup>a,\*</sup>, Kayhan Kantarlı <sup>b,1</sup>, Mehmet Yıldız <sup>c,2</sup>, Sadık Dost <sup>d,3</sup><sup>a</sup> Department of Physics, Faculty of Sciences and Arts, Adnan Menderes University, 09010-Aydın, Turkey<sup>b</sup> Department of Physics, Faculty of Sciences, Ege University, 35100-Bornova, İzmir, Turkey<sup>c</sup> Faculty of Engineering and Natural Sciences, Sabana University, 34956-Tuzla, İstanbul, Turkey<sup>d</sup> Crystal Growth Laboratory, University of Victoria, Victoria BC, Canada V8W 3W2

### ARTICLE INFO

PACS:  
71.20.Nr  
78.20.-e  
78.20.Ci

#### Keywords:

Silicon-germanium  
Dielectric function  
Spectroscopic ellipsometry  
Reflectance  
Interband transition energy

### ABSTRACT

In this article, we present measurements for the pseudo-optical functions of germanium-rich  $\text{Si}_x\text{Ge}_{1-x}$  ( $0.000 \leq x \leq 0.100$ ) single-crystals (grown by Liquid Phase Diffusion; LPD) using spectroscopic ellipsometry and photoreflectance techniques in the energy range of 1.72–3.20 eV. The  $E_1$  interband transition energies are obtained from numerically differentiated optical spectra for various crystal compositions. It was shown that the values of  $E_1$  interband transition energy determined by both the ellipsometric and photoreflectance measurements for germanium-rich  $\text{Si}_x\text{Ge}_{1-x}$  single-crystals are in agreement with those of bulk SiGe crystals reported in the literature [21–24]. The interband transition energies are found to be in the range of 2.100 and 2.215 eV for the composition values of  $0.000 \leq x \leq 0.100$ . The surface morphology of the crystals assayed via atomic force microscopy shows fibrous surfaces with the average grain size of 250 nm. The measured root-mean-square (rms) roughness and maximum height are in the range of 3.78–5.40 and 32.42–67.84 nm, respectively, with increasing germanium composition.

© 2009 Elsevier Ltd. All rights reserved.

### 1. Introduction

The binary alloy system  $\text{Si}_x\text{Ge}_{1-x}$  provides a continuous series of single crystals with gradually varying electrical and optical properties in accordance with the needs of device applications. In this article, it is to be noted that we have used the term crystal and alloy interchangeably.  $\text{Si}_x\text{Ge}_{1-x}$  single crystals for device applications have generally been prepared in the form of thin films grown on a silicon substrate by various epitaxial growth techniques [1–4]. However, in these growth techniques

the alloy layer is compressively strained and a high density of misfit dislocations is invariably created at the interface of the  $\text{Si}_x\text{Ge}_{1-x}$  and Si when the thickness of the strained layer exceeds a critical thickness. The existence of these dislocations reduces the mobility and electronic quality of semiconductor single crystal materials [5]. The critical layer thickness decreases significantly with increasing germanium content, whereas most of the applications require a much thicker  $\text{Si}_x\text{Ge}_{1-x}$  layer with higher germanium content.

In order to grow high quality  $\text{Si}_x\text{Ge}_{1-x}$  single crystals with uniform compositions, a large number of crystal growth techniques such as Czochralski (Cz) [6–9], floating zone (FZ) [10], Bridgman [11,12], multi-component [13] and liquid encapsulated zone melting [14] have been utilized. Nevertheless, many of these methods did have limited success in terms of growing compositionally uniform and low defect density crystals. Because of the large miscibility gap, which leads to segregation

\* Corresponding author. Tel.: +90 256 2137607; fax: +90 256 2135973.

E-mail addresses: [hderin@adu.edu.tr](mailto:hderin@adu.edu.tr) (H. Derin),[kayhan.kantarli@ege.edu.tr](mailto:kayhan.kantarli@ege.edu.tr) (K. Kantarlı),[meiyildiz@sabanciuniv.edu](mailto:meiyildiz@sabanciuniv.edu) (M. Yıldız), [sdost@me.uvic.ca](mailto:sdost@me.uvic.ca) (S. Dost).<sup>1</sup> Tel.: +90 232 3884000; fax: +90 232 3881036.<sup>2</sup> Tel.: +90 216 4839517; fax: +90 216 4839550.<sup>3</sup> Tel.: +1 250 7218898; fax: +1 250 7216294.

coefficients far from unity, any small changes in the solidification rate can result in significant compositional variations and in turn various types of defects in the grown crystals. Thus, the crystal growth method to be chosen is of a crucial importance to obtain bulk  $\text{Si}_x\text{Ge}_{1-x}$  single crystals with desired qualities.

It has been shown that “Liquid Phase Diffusion” (LPD) technique developed by Nakajima et al. [13] and Azuma et al. [15] and improved also by the studies of Yıldız et al. [16] and Yıldız and Dost [17] based on two-and three-dimensional computational models has a promising capacity to produce high quality and compositionally uniform SiGe single crystals. Another advantage of the LPD technique is its relative simplicity and low capital cost to grow large size  $\text{Si}_x\text{Ge}_{1-x}$  single crystals with a wide composition. In this technique the solvent material (Ge) is sandwiched between a single crystal substrate (seed, Ge) and polycrystalline source material (feed, Si). In that sense, the LPD technique is considered to be a solution growth method [16].

The availability of optical properties of  $\text{Si}_x\text{Ge}_{1-x}$  crystals is crucial for the design of optical devices. In particular, the composition dependence of the optical absorption spectrum is very useful in identifying inter-band transitions. Several studies on the optical properties of germanium-rich SiGe/Si layers grown by various growth techniques such as atmospheric remote plasma chemical vapor deposition (RPCVD) [18], low-pressure vapor phase epitaxy (LPVPE) [19,20], liquid-phase epitaxy (LPE) [21] and Czochralski (Cz) [22], have been carried out. However, the optical constants and dielectric functions of  $\text{Si}_x\text{Ge}_{1-x}$  single crystals with higher Ge contents ( $0.000 \leq x \leq 0.100$ ) grown by the liquid phase diffusion (LPD) technique have not been reported yet in the literature.

In this study, we have measured the pseudo-optical functions of Ge-rich  $\text{Si}_x\text{Ge}_{1-x}$  ( $0.000 \leq x \leq 0.100$ ) single-crystals grown by LPD technique in the energy range of 1.72–3.20 eV using spectroscopic ellipsometry (SE). The optical reflectance of test samples has also been measured in the same energy region by spectrophotometric technique. The compositions of the grown single crystals are correlated with results of both the SE and the reflectance methods. Our analysis shows that the optical spectra of germanium-rich  $\text{Si}_x\text{Ge}_{1-x}$  single crystals determined by SE and reflectance techniques are in agreement with those of the relaxed SiGe alloys reported in the literature [21–24]. The surface morphology of test samples examined via AFM shows fibrous surfaces with the average grain size of 250 nm. The measurement rms roughness and maximum height are in the range of 3.78–5.40 and 32.42–67.84 nm, respectively, with increasing germanium composition.

## 2. Materials preparation and measurement methods

The bulk  $\text{Si}_x\text{Ge}_{1-x}$  single-crystals were grown by the LPD technique. The details of the growth process and the composition measurement are described in Ref. [16]. Grown crystals have cylindrical form with the diameter of 25 mm and the height of 20–25 mm. For the compositional analysis and the delineation of single crystallinity, grown crystals were bisected along the growth axis.

A 2-mm-thick plate was cut out of the first half to determine axial and radial compositional distributions of silicon. The cut samples were polished using SiC papers of 1200 mesh size followed by diamond suspensions of 6 and 1  $\mu\text{m}$  particle size sequentially and then were etched at room temperature in the mixture of HF (49%): $\text{H}_2\text{O}_2$  (30%): $\text{H}_2\text{O}$  with the ratio of 1:1:4 for 12–15 min to delineate the extent of single crystallinity and growth striations. The compositions of the grown single crystals were measured at various axial and radial locations by Electron Probe Microanalysis (EPMA) and Energy Dispersive X-ray Analysis (EDX) with the acceleration voltage of 20 kV and SiK 1.739 keV and GeK 9.873 keV peaks [16]. Grown crystals have highly uniform radial compositional distribution as reported in Ref. [16]. For the optical measurements, test sample layers are extracted from the bisected grown crystals by cutting them perpendicular to the growth axis. The thicknesses of the cut SiGe layers are approximately 3.5 mm for all the composition values,  $x=0.000$ , 0.026 and 0.100. The above described surface preparation procedure has also been used for the samples of optical measurements except for the etching stage.

The surface morphology of  $\text{Si}_x\text{Ge}_{1-x}$  single crystals for different Ge compositions was examined with a Solver P47 H atomic force microscope (NT-MTD) (Moscov, Russia) operating in tapping mode. Diamond-like carbon (DLC) coated NSG01.DLC silicon cantilevers (from NT-MTD) with a 2 nm tip apex curvature were used at its resonance frequency of 150 kHz. The Nova 914 software package was used to control the SPM system and for the analysis of the AFM images.

Ellipsometric data were taken with a Gaertner L119X ellipsometer equipped with a Babinet-soleil compensator. All measurements were performed at room temperature in the spectral range from 1.72 to 3.20 eV with an energy step of 0.164 eV and at the incident angle of  $70^\circ$ .

An ellipsometer measures conveniently the changes in the polarization of light resulted in reflection from a surface [25]. The quantity measured by ellipsometer is defined by the fundamental equation of ellipsometry

$$\rho = \tan(\Psi) \exp(i\Delta) \quad (1)$$

where,  $\tan(\psi)$  and  $\Delta$  are the relative attenuation and the phase shift difference, respectively, experienced upon reflection by the components of the electric field vector parallel and perpendicular to the plane of incidence. The measured quantity  $\rho$  depends on the complex refractive index of the absorbing bare medium under study by equation

$$\tilde{n} = n - ik = n_1 \tan\phi_1 \left[ 1 - \frac{4\rho \sin^2\phi_1}{(\rho + 1)^2} \right]^{1/2}, \quad (2)$$

where  $n$  and  $k$  are the real and imaginary parts of the complex refractive index, respectively. Also,  $n_1$  and  $\phi_1$  are the refractive index of the medium above the sample surface and the angle of incidence in the given order. The surfaces of the samples under study may be covered with various contaminants such as oxidized layers and may be microscopically rough as a result of cleaning and polishing processes. In this case the  $n$ ,  $k$  optical constants calculated

from Eqs. (1) and (2) may be considerably in error. Therefore, the optical properties of the test sample are defined by pseudo-optical function,  $\langle \tilde{n} \rangle$ , which necessarily is an average of optical responses of substrate and possible overlayer effects [26,27]. The pseudo-optical constants  $\langle n \rangle$  and  $\langle k \rangle$  of the bulk  $\text{Si}_x\text{Ge}_{1-x}$  single-crystals are computed using Eq. (2). An alternative way of expressing the ellipsometric data is the pseudo-dielectric function  $\langle \tilde{\epsilon} \rangle$ . This quantity is related to the optical constants by equation

$$\langle \tilde{\epsilon} \rangle = \langle \epsilon_1 \rangle - i\langle \epsilon_2 \rangle = [\langle n \rangle - i\langle k \rangle]^2, \quad (3)$$

where  $\langle \epsilon_1 \rangle = \langle n \rangle^2 - \langle k \rangle^2$ ;  $\langle \epsilon_2 \rangle = 2\langle n \rangle \langle k \rangle$  are the real and imaginary parts of the complex pseudo-dielectric function, respectively.

The optical reflectance spectra were recorded using a Shimadzu UV-160A spectrophotometer equipped with a reflectance attachment having an incident angle of  $5^\circ$ . The spectrophotometer has a measurement step and a wavelength resolution of 0.1 nm and  $\pm 0.5$  nm, respectively. Its measurement accuracy is fairly high, about 0.1%.

### 3. Results and discussion

The surface morphologies of the  $\text{Si}_x\text{Ge}_{1-x}$  ( $0.000 \leq x \leq 0.100$ ) single crystals used in the optical characterization process were assayed by AFM. Fig. 1(a), (b) and (c), shows the AFM images of the Si-Ge single crystal surfaces for Ge compositions  $x=0.000$ , 0.026 and 0.100, respectively. A scan across various regions of the Si-Ge single crystal surfaces shows uniform application with a root-mean-square (rms) roughness and a maximum height in the range of 3.78–5.40 nm and 32.42–67.84 nm, respectively, with increasing Ge composition. These surfaces have a fibrous structure with the average grain size of 250 nm.

Figs. 2 and 3 show the real and imaginary parts of complex refractive index, respectively, as a function of photon energy for bulk  $\text{Si}_x\text{Ge}_{1-x}$  ( $0.000 \leq x \leq 0.100$ ) single crystals. As expressed in Ref. [28], the shape of dispersion curves of the pseudo-optical constants is similar for all the three compositions studied. As seen from Fig. 2, the dispersion curves of pseudo-refractive indices  $\langle n \rangle$  have a characteristic peak that is related to interband transition energies [29]. The peak positions are at the energy range of 1.938–2.033 eV (640–610 nm). As the germanium concentration increases, peak heights decrease and the peak positions partially shift towards the lower photon energy. As for the dispersion curves of the imaginary part of the refractive index in Fig. 3,  $\langle k \rangle$  values monotonically increase until reaching 2.110–2.220 eV energy values that correspond to interband transition energies for different compositions. Above these energy levels, the imaginary part of the refractive index  $\langle k \rangle$  remains nearly constant. A similar behavior for the variation of the refractive index  $\langle n \rangle$  and extinction coefficient  $\langle k \rangle$  as a function of photon energy has also been reported by Ygartua et al. [30] and Djurisić et al. [31].

Fig. 4 shows the plot of the real part of the pseudo-dielectric function  $\langle \epsilon_1 \rangle$ , which is computed using Eq. (3), as a function of photon energy. It should be noted that the

$\langle \epsilon_1 \rangle$  spectra exhibit a similar behavior to those of  $\langle n \rangle$ . Namely, as the germanium concentration increases, the peak of  $\langle \epsilon_1 \rangle$  partially shifts towards lower energy region and the peak value decreases.

As can be deduced from Figs. 2 and 3, the root cause of the changes in the  $\langle n \rangle$  and  $\langle k \rangle$  dispersion curves originates from the effect that the Ge-composition has on the fundamental optical properties of the material. The electronic properties of the  $\text{Si}_x\text{Ge}_{1-x}$  single crystal samples for the different germanium compositions, such as interband transition energy can be investigated by means of the imaginary part of the pseudo-dielectric function,  $\langle \epsilon_2 \rangle = \langle n \rangle \langle k \rangle$ , because it is more sensitive to extinction coefficient  $\langle k \rangle$ , which is a measure of the optical absorption, than  $\langle \epsilon_1 \rangle = \langle n \rangle^2 - \langle k \rangle^2$ .

Fig. 5 represents the  $\langle \epsilon_2 \rangle$  spectra for three different germanium compositions; namely,  $x=0.000$ , 0.026 and 0.100. The spectra have peaks corresponding to  $E_1$  interband transition energies [32], and the peak positions slightly shift towards higher energies with decreasing Ge content, as also reported in Ref. [22]. The transition energies are determined to be 2.102, 2.138 and 2.215 eV for composition values of  $x=0.000$ , 0.026 and 0.100, respectively, and well-fitted by the parabola equation that relates the variation of  $E_1$  interband transition energy with composition [21]

$$E_1(x) = 2.108 + 1.287x - 0.153x(1 - x), \quad (4)$$

where  $E_1$  is given in eV. Thus, the positions of the  $E_1$  interband transition energies can provide an alternative way to determine the crystal compositions, whereby enabling SE technique to be used for the stoichiometry determination.

It appears that the spectral behavior of the real and imaginary parts of dielectric function presented in this paper is similar to those reported by Humlicek et al. [21] and Djurisić et al. [31]. However, there is a considerable difference between the numerical values. This difference might be attributed to following reasons; first, our samples were extracted from bulk single crystals with gradually varying silicon composition along the growth direction (direction perpendicular to sample surfaces). Therefore, the light experiences different compositional values as it penetrates through the surface of the sample. Second, the crystal quality, and the degree of single crystallinity might also contribute to this difference.

Fig. 6 shows the optical reflectance spectra of Ge-rich SiGe crystals. As seen from the figure, the general features of optical reflectance spectra are very similar to those of  $\langle \epsilon_2 \rangle$ . The shape of reflectance spectrum remains the same for all three SiGe single crystal samples studied in this work. However, the position of peaks shifts slightly towards higher energies in parallel to the increasing reflectivity with decreasing germanium composition. Using these results, one can confidently assume that the peak in the reflectance spectrum of SiGe system is related to the characteristic feature of the absorption spectrum corresponding to the interband transition energies for different compositions. The comparison of Figs. 5 and 6 suggest a fairly good agreement between ellipsometric and spectrophotometric results. Also, the shape of the

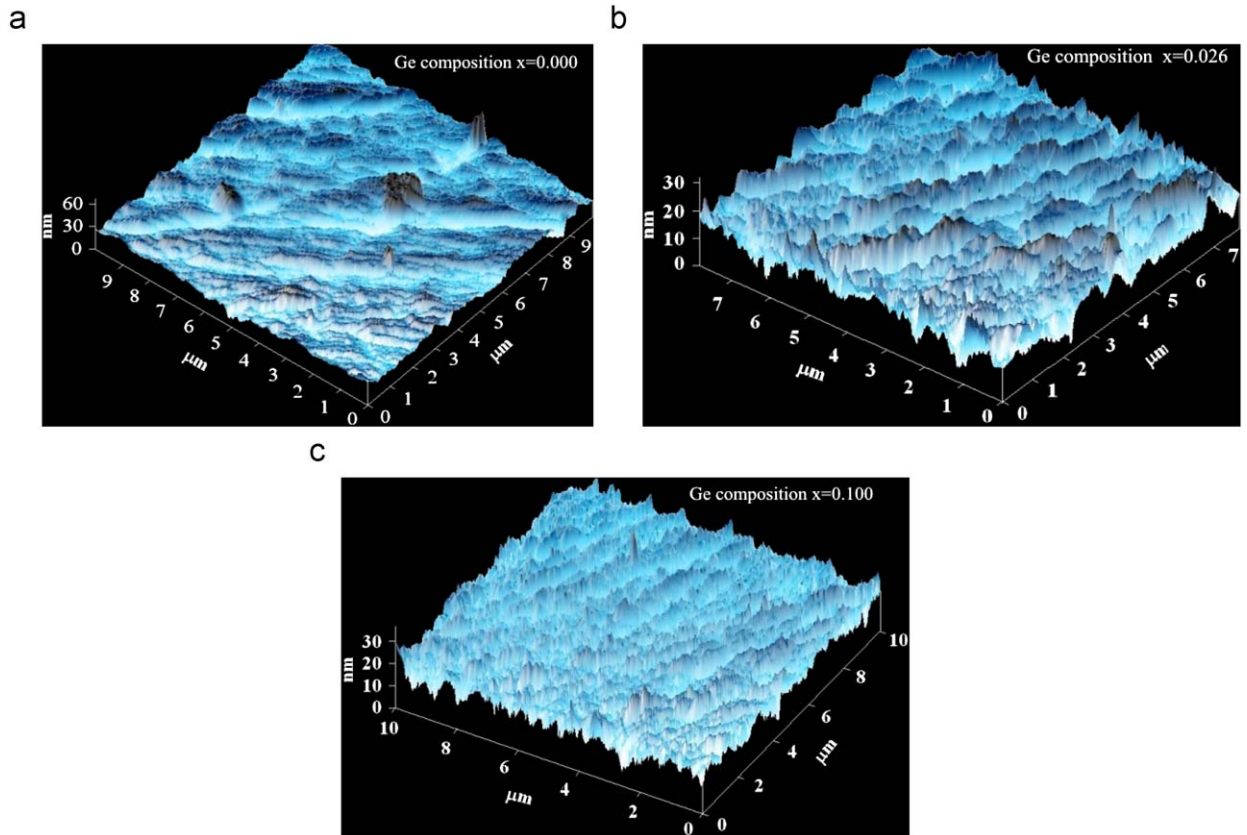


Fig. 1. Three-dimensional AFM images of the  $\text{Si}_x\text{Ge}_{1-x}$  single crystals for different germanium compositions: (a)  $x=0.000$ , (b)  $x=0.0026$  and (c)  $x=0.100$ .

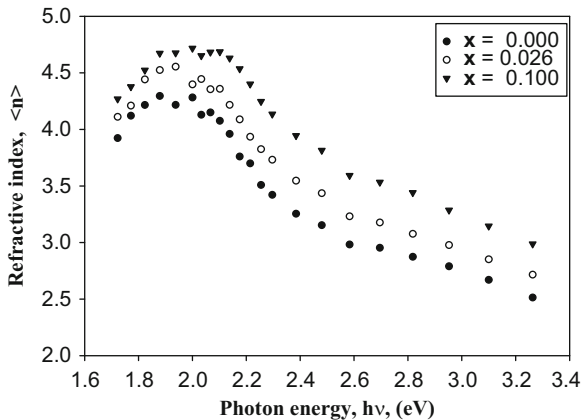


Fig. 2. Pseudo-refractive index,  $\langle n \rangle$ , dispersion for  $\text{Si}_x\text{Ge}_{1-x}$ .

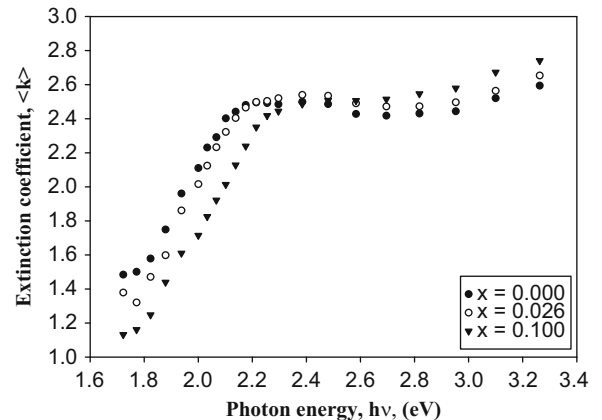


Fig. 3. Pseudo-extinction coefficient,  $\langle k \rangle$ , dispersion for  $\text{Si}_x\text{Ge}_{1-x}$ .

measured reflectance spectra agree quite well with other published results [23,24], except the splitting corresponding to the spin-orbit interaction in the reflectance maxima.

#### 4. Conclusion

We have presented pseudo-optical functions measured for  $\text{Si}_x\text{Ge}_{1-x}$  single crystal samples using ellipsometric and

spectrophotometric methods at room temperature. We have found that  $E_1$  interband transition energies corresponding to the peak values of reflectance and the imaginary part of the pseudo-dielectric function depend on the composition of material, and the values for different Ge compositions agree with the results of the SE analysis and reflectance measurements. Therefore, both the spectral and composition dependences of the optical parameters are expected to be useful in the optical

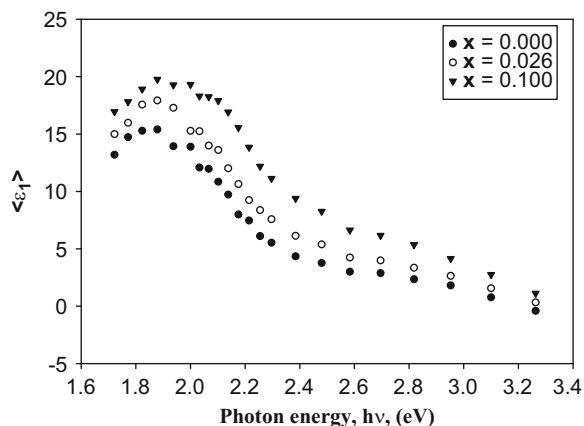


Fig. 4. Real part of the pseudo-dielectric function,  $\langle \epsilon_1 \rangle$ , of the  $\text{Si}_x\text{Ge}_{1-x}$  single crystals as a function of the photon energy for different germanium compositions.

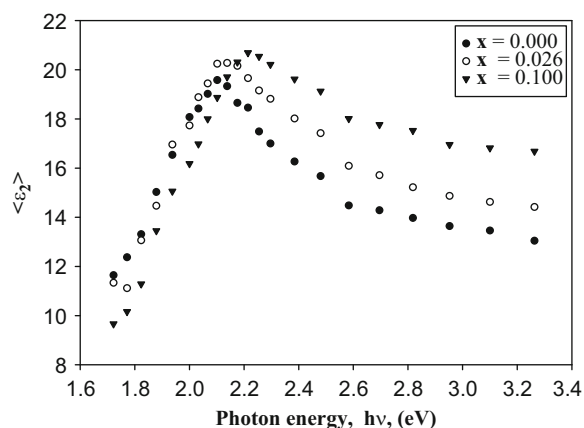


Fig. 5. Imaginary part of the pseudo-dielectric function,  $\langle \epsilon_2 \rangle$ , of the  $\text{Si}_x\text{Ge}_{1-x}$  single crystals as a function of the photon energy for different germanium compositions.

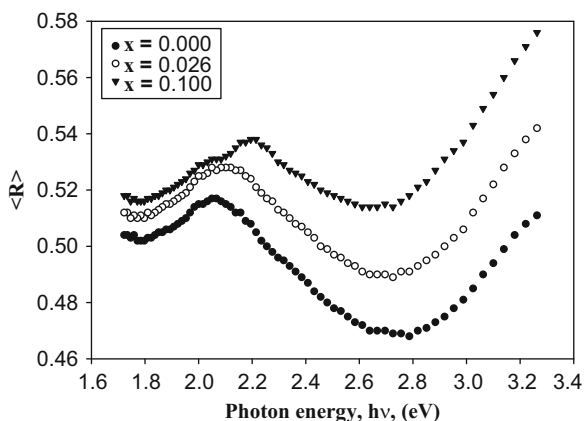


Fig. 6. Reflectance spectra of the  $\text{Si}_x\text{Ge}_{1-x}$  single crystals for different germanium compositions.

characterization of SiGe-based structures. These data of optical characterization verify LPD technique is convenient in growing high quality, compositionally uniform and

Ge-rich SiGe seed single crystals required in many device applications and the LPEE technique. Furthermore, because of the high accuracy of spectral positions determined by ellipsometric and reflectance measurements in general and the large slope of  $E_1$  peak in  $\text{Si}_x\text{Ge}_{1-x}$  in particular, both the techniques can be a good tool of quality control for such new materials even in the industrial lines.

## Acknowledgements

The authors are thankful to Assoc. Prof. Dr. Salih Okur from Department of Physics, Faculty of Science, İzmir Institute of Technology, İzmir, Turkey, for permitting the use of the AFM device.

## References

- [1] Luo YH, Wan J, Forrest RL, Liu JL, Goorsky MS, Wang KL. *J Appl Phys* 2001;89(12):8279–83.
- [2] Fitzgerald AE, Xie YH, Green ML, Brasen D, Kortan AR, Michel J, Mii Y-J, Weir BE. *Appl Phys Lett* 1991;59(7):811–3.
- [3] Bhattacharya P, Singh J, Gular I. E. Final Technical Report, Department of Electrical Engineering and Computer Science, The University of Michigan, USA, 1997.
- [4] Meyerson BS, Ismail KE, Harame DL, LeGoues FK, Stork JMC. *Semiconduct Sci Technol* 1994;9(11):2005–10.
- [5] Paul DJ. *Adv Mater* 1999;11(3):191–204.
- [6] Abrasimov NV, Rossolenko SN, Thieme W, Gerhardt A, Schroder W. *J Cryst Growth* 1997;174(1-4):182–6.
- [7] Matsui A, Yonenaga I, Sumino K. *J Cryst Growth* 1998;183(1-2):109–116.
- [8] Kaurten M, Schilz J. *J Cryst Growth* 1994;139(1-2):1–5.
- [9] Yonenaga I, Nonaka M. *J Cryst Growth* 1998;191(3):393–8.
- [10] Wollweber J, Schulz D, Schroder W. *J Cryst Growth* 1996;163(3):243–8.
- [11] Dold P, Barz A, Recha S, Pressel K, Franz M, Benz KW. *J Cryst Growth* 1998;192(1-2):125–35.
- [12] Dahlen A, Fattah A, Hanke G, Karthaus E. *Cryst Res Technol* 1994;29(2):187–98.
- [13] Nakajima K, Kodama S, Miyashita S, Sazaki G, Hiyamizu S. *J Cryst Growth* 1999;205(3):270–6.
- [14] Bliss D, Demczyk B, Anselmo A, Bailey J. *J Cryst Growth* 1997;174(1-4):187–93.
- [15] Azuma Y, Usami N, Ujihara T, Sazaki G, Murakami Y, Miyashita S, Fujiwara K, Nakajima K. *J Cryst Growth* 2001;224(3-4):204–11.
- [16] Yıldız M, Dost S, Lent B. *J Cryst Growth* 2005;280(1-2):151–60.
- [17] Yıldız M, Dost S. *Int J Eng Sci* 2005;43:1059–80.
- [18] Lee H. *Thin Solid Films* 1998;313-314:167–71.
- [19] Pickering C, Carline RT, Robbins DJ, Leong WY, Barnett SJ, Pitt AD, Cullis AG. *J Appl Phys* 1993;73(1):239–50.
- [20] Carline RT, Pickering C, Robbins DJ, Leong WY, Pitt AD, Cullis AG. *Appl Phys Lett* 1994;64(9):1114–6.
- [21] Humlicek J, Garriga M, Alonso MI, Cardona M. *J Appl Phys* 1989;65(7):2827–32.
- [22] Humlicek J, Lukes F, Schmidt E, Kekoua MG, Khoutsishvili E. *Phys Rev B* 1986;33(2):1092–101.
- [23] Tauc J, Abraham A. *J Phys Chem Solids* 1961;20(3-4):190–2.
- [24] Schmidt E. *Phys Status Solidi* 1968;27:57–66.
- [25] Azzam RMA. *Ellipsometry and Polarized Light*. Amsterdam: North-Holland; 1986.
- [26] Palik ED. *Handbook of Optical Constants of Solids I*. New York: Academic Press; 1998 96.
- [27] Vedam K. *Physics of Thin Films*, Vol. 19. New York: Academic Press; 1994 57.
- [28] Palik ED. *Handbook of Optical Constants of Solids III*. New York: Academic Press; 1998 537–538.
- [29] Aspnes DE. *Handbook on Semiconductors*, Vol. 2. Amsterdam: North-Holland; 1980.
- [30] Ygartua C, Liaw M. *Thin Solid Films* 1998;31–314:237–42.
- [31] Djuricic AB, Li EH. *Semiconduct Sci Technol* 2001;16:59–65.
- [32] Kline JS, Pollak FH, Cardona M. *Helv Phys Acta* 1968;41:968–76.